

Synchronization of coupled nonlinear oscillatiors with gamma-distributed delays

Irinel-Constantin Morarescu, Wim Michiels, Marc Jungers

▶ **To cite this version:**

Irinel-Constantin Morarescu, Wim Michiels, Marc Jungers. Synchronization of coupled nonlinear oscillatiors with gamma-distributed delays. American Control Conference, ACC 2013, Jun 2013, Washington, United States. pp.CDROM. hal-00783112

HAL Id: hal-00783112
https://hal.science/hal-00783112

Submitted on 31 Jan 2013

HAL is a multi-disciplinary open access archive for the deposit and dissemination of scientific research documents, whether they are published or not. The documents may come from teaching and research institutions in France or abroad, or from public or private research centers.

L'archive ouverte pluridisciplinaire **HAL**, est destinée au dépôt et à la diffusion de documents scientifiques de niveau recherche, publiés ou non, émanant des établissements d'enseignement et de recherche français ou étrangers, des laboratoires publics ou privés.

Synchronization of coupled nonlinear oscillators with shifted gamma-distributed delays

Irinel-Constantin Morărescu[#] Wim Michiels[†] Marc Jungers[#]

***Abstract*— We derive conditions for the synchronization of coupled nonlinear oscillators affected by distributed delays in the interconnections. The distributed delays are characterized by a gamma-distribution kernel with a gap. The approach is based on the stability analysis of synchronized equilibria in the (delays,gain) parameter space and the characterization of the structure of the emanating solutions at the bifurcations. The results are applied to networks of coupled Lorenz system. In particular it is shown that, independently of the network topology, for sufficiently large coupling gains the distribution of the delay has a stabilizing effect on the stability of the synchronized equilibrium.**

***Index Terms*— Coupled oscillators, distributed delays, synchronization, delayed couplings**

I. Introduction

Systems of coupled nonlinear oscillators have been used to describe a variety of phenomena in different fields of science ranging from electric network modeling to brain activity behavior. The emergence of synchronization in networks of oscillators with couplings given by various types of topologies has received much attention [2], [9], [11]. The influence of discrete fixed delays on the consensus and synchronization of coupled subsystems is considered in [8], [5], [7]. However, as pointed out in several studies [3], [1], [4], the behavior of interconnected systems is often more accurately reflected by considering distributed delays affecting their interactions.

This paper focuses on the synchronization problem in networks of identical oscillators with couplings affected by distributed delays. Throughout the study we consider a set of p identical oscillators coupled via a fixed, directed network topology. Each oscillator has a behavior described by the following nonlinear dynamics

$$\dot{x}_i(t) = f(x_i(t)) + Bu_i(t),\ y_i(t) = Cx_i(t),\ i = 1, \dots, p \tag{1}$$

where $x_i \in \mathbb{R}^{n_x},\ i = 1, \dots, p,\ B, C^\top \in \mathbb{R}^{n_x \times m}$, and $f : \mathbb{R}^n \mapsto \mathbb{R}^n$ is twice continuously differentiable.

Assumption 1: We assume that for $u_i = 0$ the system has at least one unstable equilibrium of focus type, which we denote by x^* in what follows.

The network topology is described by the directed graph

$$\mathcal{G}(V, E, \mathbb{G}) \tag{2}$$

characterized by the node set $V = \{1, \dots, p\}$, a set of edges E where $(k, l) \in E$ if and only if $\alpha_{k,l} \neq 0$, and a weighted adjacency matrix $\mathbb{G}$ with zero diagonal entries and non-diagonal entries equal to $\alpha_{k,l}$. Obviously, each vertex corresponds to an oscillator and the edges describe the coupling strength between them. Precisely, we couple the systems (1) by means of the control law

$$u_i(t) = k\left(\sum_{l=1}^{p} \alpha_{i,l} \int_0^\infty g(\theta)(y_l(t-\theta) - y_i(t))\mathrm{d}\theta\right), \quad i = 1, \dots, p, \tag{3}$$

where $k > 0$ represents the gain parameter and $g(\cdot)$ stands for the gamma-distributed delay with a gap kernel given by

$$g(\xi) = \begin{cases} 0, & \xi < \tau, \\ \frac{(\xi-\tau)^{n-1} \mathrm{e}^{-\frac{\xi-\tau}{T}}}{T^n (n-1)!}, & \xi \geq \tau, \end{cases} \tag{4}$$

where $n \in \mathbb{N},\ T > 0$ and $\tau \geq 0$. Note that $g(\xi) \geq 0$ for all $\xi \geq 0$ and $\int_0^\infty g(\xi) d\xi = 1$. A motivation for the consideration of this type of delay distribution can be found in [6].

The coupled system (1)-(3) has an equilibrium

$$(x^*, \dots, x^*) \in \mathbb{R}^{n \times p}, \tag{5}$$

which we denote the synchronized equilibrium. In what follows we perform a stability analysis of the equilibrium (5) in the parameter space (k, T, τ), characterize the emanating solutions in the bifurcations and apply these results to networks of coupled Lorenz systems.

II. Preliminaries

The following assumptions are supposed to hold.

Assumption 2: The graph $\mathcal{G}$ is strongly connected.

Assumption 3: The adjacency matrix G is stochastic i.e.

$$\sum_{l=1}^{p} \alpha_{i,l} = 1, \quad i = 1, \dots, p.$$

The first assumption is natural in the context of synchronization while the second assumption will be motivated in the sequel.

We recall that Perron-Frobenius theorem for stochastic matrices assures that

1) G has a simple eigenvalue equal to 1 and $[1, \dots, 1]^\top$ is the corresponding right-eigenvector.
2) The left eigenvector $\gamma = [\gamma_1, \dots, \gamma_p]$ associated with the eigenvalue 1 may be chosen such that $\gamma_i > 0,\ 1 \leq i \leq p$ and $\sum_{i=1}^{p} \gamma_i = 1$.

[#] Université de Lorraine, CRAN, UMR 7039, 2 Avenue de la Forêt de Haye, France and the CNRS, CRAN, UMR 7039, constantin.morarescu@univ-lorraine.fr, marc.jungers@univ-lorraine.fr

[†]Department of Computer Science, Katholieke Universiteit Leuven, Celestijnenlaan 200A, 3001 Heverlee, Belgium Wim.Michiels@cs.kuleuven.be

3) All eigenvalues of G have modulus smaller than or equal to 1.

In what follows we denote the eigenvalues of G as $\lambda_i(G),\ i = 1, \ldots, p$, where we take the following convention.

Convention 1: $\lambda_1(G) = 1$.

Following the coordinate transformation in [5] we can bring the system (1) and (3) in the form

$$\begin{aligned}
\dot{x}_1(t) &= f(x_1(t)) \\
&\quad + BkC\left(\sum_{l=1}^{p}\alpha_{1,l}\right)\int_0^\infty g(\theta)(x_1(t-\theta)-x_1(t))\mathrm{d}\theta \\
&\quad + BkC\sum_{l=1}^{p}\alpha_{1,l}\int_0^\infty g(\theta)e_l(t-\theta)\mathrm{d}\theta,
\end{aligned}$$

$$\begin{aligned}
&\begin{bmatrix} \dot{e}_2(t) \\ \vdots \\ \dot{e}_p(t) \end{bmatrix} = \begin{bmatrix} f(x_1(t)+e_2(t)) - f(x_1(t)) \\ \vdots \\ f(x_1(t)+e_p(t)) - f(x_1(t)) \end{bmatrix} - \\
&k\left(\begin{bmatrix} \sum_{l=1}^{p}\alpha_{2,l} & & \\ & \ddots & \\ & & \sum_{l=1}^{p}\alpha_{p,l} \end{bmatrix} \otimes BC\right)\begin{bmatrix} e_2(t) \\ \vdots \\ e_p(t) \end{bmatrix} \\
&+ k\tilde{G}\otimes BC\begin{bmatrix} \int_0^\infty g(\theta)e_2(t-\theta)\mathrm{d}\theta \\ \vdots \\ \int_0^\infty g(\theta)e_p(t-\theta)\mathrm{d}\theta \end{bmatrix} - \\
&\left(k\begin{bmatrix} \sum_{l=1}^{p}\alpha_{1,l} - \sum_{l=1}^{p}\alpha_{2,l} \\ \vdots \\ \sum_{l=1}^{p}\alpha_{1,l} - \sum_{l=1}^{p}\alpha_{p,l} \end{bmatrix} \otimes BC\right)\cdot \\
&\int_0^\infty g(\theta)(x_1(t-\theta)-x_1(t))\mathrm{d}\theta,
\end{aligned} \tag{6}$$

where $e_i = x_i - x_1,\ i = 2, \ldots, p$. As in [5], Assumption 3 guarantees the existence of synchronized solutions ($e_2 = \ldots = e_p = 0$ implies $\dot{e}_2 = \ldots \dot{e}_p = 0$).

III. Stability analysis of synchronized equilibria

Linearizing the system (1) and (3) around the synchronized equilibrium $(x^*, \ldots, x^*)$, we obtain

$$\begin{aligned}
\begin{bmatrix} \dot{v}_1(t) \\ \vdots \\ \dot{v}_p(t) \end{bmatrix} &= I\otimes(A-BkC)\begin{bmatrix} v_1(t) \\ \vdots \\ v_p(t) \end{bmatrix} \\
&\quad + kG\otimes BC\begin{bmatrix} \int_0^\infty g(\theta)v_1(t-\theta)d\theta \\ \vdots \\ \int_0^\infty g(\theta)v_p(t-\theta)d\theta \end{bmatrix},
\end{aligned} \tag{7}$$

where $A = \dfrac{\partial f}{\partial x}(x^*)$.

A. Characteristic equation

The characteristic function of (7) is given by

$$f(s,k,T,\tau) = \det F(s,k,T,\tau), \tag{8}$$

where the characteristic matrix F is defined by

$$F(s,k,T,\tau) = I\otimes(sI - A + kBC) - G\otimes kBC\frac{e^{-s\tau}}{(1+sT)^n}. \tag{9}$$

Using the factorization $G = P\Lambda P^{-1}$, where $\Lambda \in \mathbb{C}^{p\times p}$ is triangular and $P \in \mathbb{C}^{p\times p}$, the characteristic function may be decomposed as

$$f(s,k,T,\tau) = \prod_{i=1}^{p} f_i(s,k,T,\tau), \tag{10}$$

where

$$\begin{aligned}
&f_i(s,k,T,\tau) = \det F_i(s,k,T,\tau), \\
&F_i(s,k,T,\tau) = sI - A + kBC - kBC\lambda_i(G)\frac{e^{-s\tau}}{(1+sT)^n}, \\
&\qquad i = 1, \ldots, p.
\end{aligned} \tag{11}$$

We note that each function $f_i(s,k,T,\tau)$ may be rewritten

$$f_i(s,k,T,\tau) = \sum_{l=0}^{p} Q_l(s,k)\left(\frac{e^{-s\tau}}{(1+sT)^n}\right)^l \tag{12}$$

where $Q_l,\ l = 1, \ldots, p$, are polynomials satisfying

$$\deg Q_0(s) > \deg Q_l(s), \quad l = 1, \ldots, p. \tag{13}$$

B. Eigenspaces and behavior on the onset of instability

We investigate the eigenspace of the characteristic matrix (9), corresponding to a characteristic root. For reasons of simplicity we restrict ourselves to the generic case where all the eigenvalues of the adjacency matrix G are simple. Let E_i be the eigenvector of G corresponding to the eigenvalue $\lambda_i(G),\ i = 1, \ldots, p$.

If for some $l \in \{1, \ldots, p\}$, the equation

$$f_l(s,k,T,\tau) = 0$$

has a simple root at $s = \hat{s}$ such that

$$F_l(\hat{s},k,T,\tau)\ V = 0, \quad V \in \mathrm{C}^{n\times 1}, \tag{14}$$

then it can be verified that

$$F(\hat{s},k,T,\tau)\ (E_l\otimes V) = 0. \tag{15}$$

This implies that the linearized system (7) has an exponential solution

$$\begin{bmatrix} \nu_1(t) \\ \vdots \\ \nu_p(t) \end{bmatrix} = c(E_l\otimes V)e^{\hat{\lambda}t} = c\begin{bmatrix} e_{l,1}V \\ \vdots \\ e_{l,p}V \end{bmatrix}e^{\hat{\lambda}t}, \tag{16}$$

with the constant c depending on the initial conditions. In words, in an exponential solution of (7) corresponding to a zero of $f_l(s,k,T,\tau)$, the relation between the state variables

of an individual subsystem is determined by the null vector of F_l, while the relation between the corresponding state variables of the different subsystems is *solely* determined by the eigenvector E_l, corresponding to the l-th eigenvalue of the adjacency matrix G. This implies that all modes can be classified in at most p types, based on the relations between the behavior of the different subsystems. Note for example that bifurcations of the synchronized equilibrium due to imaginary axis zeros of f_1 are bifurcations where the synchronized behavior is preserved in the emanating solution, as $E_1 = [1\ 1\ \cdots\ 1]^T$.

C. Stability crossing curves in the delay parameters space

For a fixed $k = k^*$ we describe the *stability crossing curves* $\mathcal{T}$, which is the set of (T, τ) values such that (8) has imaginary axis solutions.

As the parameters (T, τ) cross the stability crossing curves, some characteristic roots cross the imaginary axis. Therefore, the number of roots on the right half complex plane are different on the two sides of the curves, from which we may describe the parameter regions of (T, τ) in $\mathbb{R}^2_+$ for the system to be stable.

Another related useful concept is the frequency *crossing set* Ω, which is defined as the collection of all $\omega > 0$ such that there exists a parameter pair (T, τ) such that $f(j\omega, k^*, T, \tau) = 0$. In other words, as the parameters T and τ vary, the characteristic roots may cross the imaginary axis at $j\omega$ if and only if $\omega \in \Omega$.

Proposition 1: The crossing set Ω consists of a finite number of bounded intervals, Ω_1, Ω_2, ..., Ω_N.

Proof: Due to decomposition (10) we may reduce the study of $f(j\omega, k^*, T, \tau) = 0$ to the study of $f_i(j\omega, k^*, T, \tau) = 0$. Therefore we have to study the crossing set of functions given by (12). Since $1 + j\omega T \neq 0$ the equation $f_i(j\omega, k^*, T, \tau) = 0$ can be rewritten as

$$Q_0(j\omega, k^*)(1+j\omega T)^{pn} = -\sum_{l=1}^{p} Q_l(s, k^*)e^{-jl\omega\tau}(1+j\omega T)^{(p-l)n}$$

Taking the modulus in the previous equation one gets

$$\mid Q_0(j\omega, k^*) \mid \mid 1+j\omega T \mid^{pn} \leq \sum_{l=1}^{p} \mid Q_l(s, k^*) \mid \mid 1+j\omega T \mid^{(p-l)n}$$

Using $\mid 1 + j\omega T \mid \geq 1$ one can multiply each terms in the right hand side with powers of $\mid 1 + j\omega T \mid$ to obtain

$$\mid Q_0(j\omega, k^*) \mid \leq \sum_{l=1}^{p} \mid Q_l(s, k^*) \mid . \tag{17}$$

In conclusion $\omega \in \Omega$ implies that (17) is satisfied. The assertion follows from (13). ∎

Proposition 2: Given any $\omega > 0$, $\omega \in \Omega$, all the corresponding T, τ satisfying $f_i(j\omega, k^*, T, \tau) = 0$ can be computed by

$$T = T_l = \frac{1}{\omega}\left(\mid z_l(\omega) \mid^{-2/n} -1\right)^{1/2} \tag{18}$$

$$\tau = \tau_{l,m} = \frac{1}{\omega}(-\angle z_l(\omega) - n\arctan(\omega T) + 2m\pi), \quad m = 0, \pm1, \pm2, ... \tag{19}$$

where $z_l(\omega)$ satisfies $\mid z_l(\omega) \mid < 1$ and is a solution of

$$\sum_{\ell=0}^{p} Q_\ell(j\omega, k^*)z^\ell = 0. \tag{20}$$

Proof: Let us consider the following variable transformation $z = \dfrac{e^{-j\omega\tau}}{(1+j\omega T)^n}$. Then, the equation $f_i(j\omega, k^*, T, \tau) = 0$ rewrites as

$$\sum_{l=0}^{p} Q_l(j\omega, k^*)z^l = 0$$

Solving this equation in z we get the solutions $z_1(\omega), \ldots, z_h(\omega)$. From definition, it is clear that $\mid z \mid < 1$ for any value of $\omega > 0$. Therefore, the admissible solutions are given by those $z_l(\omega)$, $l = 1, \ldots, h$ with $\mid z_l(\omega) \mid < 1$. For such z_l the corresponding pair (T, τ) can be simply computed by (18) and (19). ∎

Note that z solving (20) can be equivalently expressed as z being an eigenvalue of the pencil

$$\Lambda(z) := (-j\omega I + A - k^*BC) + z(k^*BC).$$

We will not restrict $\angle z_l(\omega)$ to a 2π range. Rather, we allow it to vary continuously within each interval Ω_i. Thus, for each fixed m and l, (18) and (19) represent a continuous curve. We denote such a curve as $\mathcal{T}_i^{l,m}$. Therefore, corresponding to a given interval Ω_i, we have an infinite number of continuous stability crossing curves $\mathcal{T}_i^{l,m}$, $m = 0, \pm1, \pm2, ...$ It should be noted that, for some m, part or the entire curve may be outside of the range $\mathbb{R}^2_+$ and, therefore, may not be physically meaningful.

The collection of all the points in $\mathcal{T}$ corresponding to Ω_i may be expressed as

$$\mathcal{T}_i = \bigcup_{m=-\infty}^{+\infty} \bigcup_{l=1}^{h} \left(\mathcal{T}_i^{l,m} \bigcap \mathbb{R}^2_+\right).$$

Obviously, $\mathcal{T} = \bigcup_{i=1}^{N} \mathcal{T}_i$.

D. Computation of the crossing direction

Let $j\omega^*$ be an imaginary axis characteristic root for parameter values $(T, \tau) = (T^*, \tau^*)$, which are lying on the stability crossing curve $\mathcal{T}_i^{l,m}$. Let r be such that $f_r(j\omega^*, k^*, T^*, \tau^*) = 0$. Introduce the following notations:

$$\begin{aligned} R_0 + jI_0 &= \frac{\partial f_r(s,k^*,T,\tau)}{\partial s}\Big|_{s=j\omega^*, T=T^*, \tau=\tau^*}, \\ R_1 + jI_1 &= \frac{\partial f_r(s,k^*,T,\tau)}{\partial T}\Big|_{s=j\omega^*, T=T^*, \tau=\tau^*}, \\ R_2 + jI_2 &= \frac{\partial f_r(s,k^*,T,\tau)}{\partial \tau}\Big|_{s=j\omega^*, T=T^*, \tau=\tau^*}. \end{aligned}$$

If matrix

$$M := \begin{bmatrix} R_1 & R_2 \\ I_1 & I_2 \end{bmatrix}$$

is invertible then, by the implicit function theorem the equations

$$\begin{cases} \Re(f_r(\sigma + j\omega, k^*, T, \tau)) = 0 \\ \Im(f_r(\sigma + j\omega, k^*, T, \tau)) = 0 \end{cases}$$

locally define a function $(\sigma,\omega)\mapsto(T,\tau)$ mapping $(0,\omega^*)$ to (T^*,τ^*) and satisfying

$$\begin{aligned}\begin{bmatrix}\frac{\partial T}{\partial\sigma}(0,\omega^*)\\ \frac{\partial\tau}{\partial\sigma}(0,\omega^*)\end{bmatrix}&=-M^{-1}\begin{bmatrix}R_0\\ I_0\end{bmatrix},\\ \begin{bmatrix}\frac{\partial T}{\partial\omega}(0,\omega^*)\\ \frac{\partial\tau}{\partial\omega}(0,\omega^*)\end{bmatrix}&=-M^{-1}\begin{bmatrix}-I_0\\ R_0\end{bmatrix}.\end{aligned}\tag{21}$$

We will call the direction of the curve $\mathcal{T}_i^{l,m}$ that corresponds to increasing ω the *positive direction*. Since the tangent of $\mathcal{T}_i^{l,m}$ along the positive direction is $\left(\frac{\partial T}{\partial\omega},\frac{\partial\tau}{\partial\omega}\right)$, the normal to $\mathcal{T}_i^{l,m}$ pointing to the left hand side of positive direction is $\left(-\frac{\partial\tau}{\partial\omega},\frac{\partial T}{\partial\omega}\right)$. Corresponding to a pair of complex conjugate solutions of (8) crossing the imaginary axis along the horizontal direction, (T,τ) moves along the direction $\left(\frac{\partial T}{\partial\sigma},\frac{\partial\tau}{\partial\sigma}\right)$. So, as (T,τ) crosses the stability crossing curve from the right hand side to the left hand side, a pair of complex conjugate solutions of (8) cross the imaginary axis to the right half plane, if

$$\left(\frac{\partial T}{\partial\omega}\frac{\partial\tau}{\partial\sigma}-\frac{\partial\tau}{\partial\omega}\frac{\partial T}{\partial\sigma}\right)_{s=j\omega}>0,\tag{22}$$

i.e. the region on the left of $\mathcal{T}_i^{l,m}$ gains two solutions on the right half plane. If the inequality (22) is reversed then the region on the left of $\mathcal{T}_i^{l,m}$ loses two right half plane solutions. Using (21) a direct computation shows that

$$\left(\frac{\partial T}{\partial\omega}\frac{\partial\tau}{\partial\sigma}-\frac{\partial\tau}{\partial\omega}\frac{\partial T}{\partial\sigma}\right)_{s=j\omega}=\frac{(R_0^2+I_0^2)(R_2I_1-R_1I_2)}{(R_1I_2-I_1R_2)^2}.$$

This brings us to the following result.

Proposition 3: Let $\omega\in\Omega_r\subset\Omega$ and $(T,\tau)\in\mathcal{T}_i$ such that $j\omega$ is a simple solution of the characteristic equation $f_r(s,k^*,T,\tau)=0$. Then as (T,τ) crosses a stability crossing curve $\mathcal{T}_i^{l,m}$ from the right-hand side to the left-hand side, a pair of solutions of (8) crosses the imaginary axis to the right, through the gate $s=\pm j\omega$ if $R_2I_1-R_1I_2>0$. The crossing is to the left if the inequality is reversed.

IV. Application to coupled Lorenz systems

In this section the nonlinear oscillators (1) are specified as Lorenz systems:

$$\begin{cases}\dot{x}_{i,1}(t) &= \sigma(x_{i,2}(t)-x_{i,1}(t)),\\ \dot{x}_{i,2}(t) &= rx_{i,1}(t)-x_{i,2}(t)-x_{i,1}(t)x_{i,3}(t)+u_{i,1}(t),\\ \dot{x}_{i,3}(t) &= -bx_{i,3}(t)+x_{i,1}(t)x_{i,2}(t)+u_{i,2}(t),\end{cases}$$

$$\begin{cases}y_{i,1}(t) &= x_{i,2}(t),\\ y_{i,2}(t) &= x_{i,3}(t)-r,\quad i=1,\dots p,\end{cases}\tag{23}$$

where $u_i=[u_{i,1}\ u_{i,2}]^T, y_i=[y_{i,1}\ y_{i,2}]^T$. The parameter values are given by

$$\sigma=10,\ r=28,\ b=8/3.\tag{24}$$

Note that for $u_i\equiv 0$ each Lorenz system has three equilibria given by

$$(0,0,0),\left(\pm\sqrt{b(r-1)},\pm\sqrt{b(r-1)},r-1\right),\tag{25}$$

the latter two corresponding to unstable foci. Thus, Assumption 1 holds. Furthermore, with the parameter values (24) it exhibits a chaotic attractor [10].

If we linearize the coupled system (23) and (3) around the synchronized equilibrium

$$(x^*,\dots,x^*),\quad x^*=(\pm\sqrt{b(r-1)},\pm\sqrt{b(r-1)},r-1),\tag{26}$$

then we obtain the linear system (7), where the matrices are specified as

$$A=\begin{bmatrix}-\sigma & \sigma & 0\\ 1 & 1 & \mp\sqrt{b(r-1)}\\ \pm\sqrt{b(r-1)} & \pm\sqrt{b(r-1)} & -b\end{bmatrix},$$

$$B=C^\top=\begin{bmatrix}0&0\\1&0\\0&1\end{bmatrix}.$$

It is easy to show that the stability of the linearized system does not depend on which equilibrium x^* in (26) is considered, Therefore, we will restrict ourselves to the one in the positive octant.

In what follows we analyze the stability properties of the synchronized equilibria (26) in the (k,T,τ) parameter space. First we study the asymptotic behavior for large values of the gain parameters in §IV-A. For the standard parameters (24) this will allow us to make assertions about stability regions, stability switches and emerging behavior, which do *not* depend on the network topology. Next we present a numerical example in §IV-B.

A. Asymptotic behavior for large gain values

For $T=0$ the behavior of the stability crossing curves for large gain values is described by the following result from [5].

Theorem 1: Consider a network of coupled Lorenz systems (23) with parameters (24) and coupling (3). Assume that $T=0$. Then there exists a number $\hat{k}>0$ and a function

$$\tau^*:\ [\hat{k},\ \infty]\to\mathbb{R}_+,\ k\mapsto\tau^*(k),\tag{27}$$

satisfying the following properties:

1) there is a constant $\tilde{k}>\hat{k}$ such that for every $k>\tilde{k}$, the synchronized equilibrium has two characteristic roots in the open right half plane for all $\tau\in[0,\ \tau^*]$, while it is asymptotically stable for $\tau\in(\tau^*,\ \tau^*+\epsilon)$, with ϵ sufficiently small;
2) at $\tau=\tau^*$ a synchronization preserving Hopf bifurcation occurs;
3) for all $k\in[\hat{k},\ \infty]$ we can factor

$$\tau^*(k)=\frac{\upsilon(k)}{k}\ \text{where}\ \lim_{k\to\infty}\upsilon(k)=0.586004.\tag{28}$$

Furthermore, the number $\hat{k}$ and the function (27) are independent of the number of subsystems and of the network topology.

The following theorem shows that the qualitative behavior for large values of k is significantly different if $T \neq 0$.

Theorem 2: Consider a network of coupled Lorenz systems (23) with parameters (24) and coupling (3). Assume that $T > 0$. Then there is a constant $\hat{k}$ such that for every $k > \hat{k}$, the synchronized equilibrium is asymptotically stable independently of $\tau \geq 0$.

Proof: Part 1: We first show that for $\tau = 0$ all characteristic roots are in left half plane for sufficiently large k.

Let $i \in \{1, \ldots, p\}$. As $k \to \infty$ the function $\dfrac{f_i(s,k,T,0)}{k^2} = \det N_i(s,k)$, with $N_i(s,k) =$

$$\begin{bmatrix} s+\sigma & -\sigma & 0 \\ -\frac{1}{k} & \frac{s+1}{k} - \left(\frac{\lambda_i(G)}{(1+st)^n} - 1\right) & \frac{\sqrt{b(r-1)}}{k} \\ -\frac{\sqrt{b(r-1)}}{k} & -\frac{\sqrt{b(r-1)}}{k} & \frac{s+b}{k} - \left(\frac{\lambda_i(G)}{(1+sT)^n} - 1\right) \end{bmatrix},$$

uniformly converges on compact subsets of $\mathbb{C}$ to the function

$$\left(1 - \frac{\lambda_i(G)}{(1+sT)^n}\right)^2 (s+\sigma). \tag{29}$$

From Rouché's theorem it follows that, as $k \to \infty$, $2n+1$ zeros of $f_i(s,k,T,0)$ converge pair-wise to the $2n+1$ zeros of (29) (taking multiplicity into account). Similarly, letting $\tilde{s} = \dfrac{s}{k}$ we get $\dfrac{f_i(\tilde{s}k,k,T,0)}{k^3} = \det(\tilde{s}I - P_i(\tilde{s},k))$, where $P_i(\tilde{s},k) =$

$$\begin{bmatrix} -\frac{\sigma}{k} & \frac{\sigma}{k} & 0 \\ \frac{1}{k} & -\frac{1}{k} + \left(\frac{\lambda_i(G)}{(1+\tilde{s}kT)^n} - 1\right) & -\frac{\sqrt{b(r-1)}}{k} \\ \frac{\sqrt{b(r-1)}}{k} & \frac{\sqrt{b(r-1)}}{k} & -\frac{b}{k} + \left(\frac{\lambda_i(G)}{(1+\tilde{s}kT)^n} - 1\right) \end{bmatrix}.$$

Thus, $\frac{f_i(\tilde{s}k,k,T,0)}{k^3}$ uniformly converges on compact sets in the $\tilde{s}$-plane to $\tilde{s}(\tilde{s}+1)^2$. Rouché's theorem then implies that for sufficiently large k the function $f_i(s,k,T,0)$ has two zeros equal to $k.\tilde{s}_{1,2}$, where

$$\lim_{k\to\infty} \tilde{s}_{1,2} = -1,$$

hence they move off the infinity without leaving the open left half plane.

The function $f_i(s,k,T,0)$ has exactly $2n+3$ zeros, induced by $\mathrm{rank}(BC) = 2$. We conclude from the previous observations that all these zeros are in the open left half plane for large k if the zeros of (29) are in the open left half plane. This is the case for $i \in \{2, \ldots, p\}$. The case $i = 1$ deserves special attention, since for $\lambda_1(G) = 1$, (29) has two (rightmost) zeros equal to zero. The latter means that two zeros of $f_1(s,k,T,0)$ approach the origin as $k \to \infty$. It remains to show that these approach the imaginary axis from the left.

With $\hat{s} = ks$ we define $g(\hat{s},k) := f_1\left(\frac{\hat{s}}{k},k,T,0\right)$. By the expansion

$$\left(\frac{1}{(1+\hat{s}T/k)^n} - 1\right) = -\frac{\hat{s}Tn}{k} + O\left(\left(\frac{\hat{s}Tn}{k}\right)^2\right)$$

and, again, an application of Rouché's theorem, it follows that, as $k \to \infty$, two zeros of $g(\cdot,k)$ converge to the finite eigenvalues of the pencil $-A + \hat{s}(Tn)BC$. With the parameters (24) these eigenvalues are given by $\hat{s}_{1,2} = \frac{1}{Tn}(-1.333 \pm 1.926j)$. We conclude that the two zeros of $f_1(s,k,T,\tau)$ that converge to the origin as $k \to \infty$ satisfy

$$s_{1,2} = \frac{1}{k}\hat{s}_{1,2} + O\left(\frac{1}{k^2}\right),$$

hence, $\Re(s_{1,2}) < 0$ for large k.

Part 2: We show that for large values of k eigenvalues cannot cross the imaginary axis when varying parameter τ. The theorem then follows from the stability for $\tau = 0$.

The equation

$$f_i(j\omega,k,T,\tau) = 0$$

is equivalent to

$$\det\left(I - (j\omega I - A + kBC)^{-1}kBC\lambda_i(G)\frac{e^{-j\omega\tau}}{(1+j\omega T)^n}\right) = 0.$$

A necessary solvability conditions is given by

$$\rho\left((j\omega I - A + kBC)^{-1}kBC\frac{\lambda_i(G)}{(1+j\omega T)^n}\right) = 1,$$

with $\rho(\cdot)$ the spectral radius. This condition is always violated for large k. Indeed, in the complex plane the nonzero eigenvalues of the matrix

$$\left(j\frac{\omega}{k}I - \frac{A}{k} + BC\right)^{-1} BC\lambda_i(G), \tag{30}$$

converge to the curve

$$\Omega \geq 0 \mapsto \frac{1}{j\Omega + 1}\lambda_i(G)$$

as $k \to \infty$, uniformly in the parameter $\omega \geq 0$. Furthermore, we have:

$$\left|\frac{1}{1+j\Omega}\lambda_i(G)\right| \leq |\lambda_i(G)| \leq 1, \quad \forall \Omega \geq 0$$

and

$$\frac{1}{|(1+j\omega T)^n|} < 1, \ \forall \omega > 0.$$

It follows that zeros on the imaginary axis are not possible for large values of k. ∎

B. Numerical example

We consider a ring topology with unidirectional coupling, described by the adjacency matrix

$$G = \begin{bmatrix} 0 & \cdots & & 0 & 1 \\ 1 & 0 & & & \\ & \ddots & \ddots & & \\ & & & 1 & 0 \end{bmatrix} \in \mathbb{R}^{p\times p}, \tag{31}$$

which has the following properties:

$$\lambda_l(G) = e^{j\frac{2\pi(l-1)}{p}}, \quad E_l = \begin{bmatrix} 1 \\ e^{-j\frac{2\pi(l-1)}{p}} \\ \vdots \\ e^{-j\frac{2\pi(p-1)(l-1)}{p}} \end{bmatrix}$$

for $l = 1, \ldots, p$.

If (14) is satisfied for $\hat{s} = j\omega,\ \omega > 0$, then the emanating solution (16) becomes

$$\begin{bmatrix} \nu_1(t) \\ \vdots \\ \nu_p(t) \end{bmatrix} = c \begin{bmatrix} V\ e^{j\omega t} \\ V\ e^{j\omega t - \frac{2\pi(l-1)}{p}} \\ V\ e^{j\omega t - \frac{4\pi(l-1)}{p}} \\ \vdots \\ V\ e^{j\omega t - \frac{2(p-1)\pi(l-1)}{p}} \end{bmatrix}. \qquad (32)$$

It can be interpreted as a traveling wave solution, where the agents follow each other with a phase shift of $360(l-1)/p$ degrees. Therefore, if the characteristic root $\hat{s}$ on the imaginary axis corresponds to a Hopf bifurcation of the original nonlinear system (23) and (3) for a critical value of some free parameter, we refer to this bifurcation as a "Hopf $360(l-1)/p$" bifurcation.

For $p = 4$ subsystems the stability regions in the (k, τ) parameter space are displayed in Figure 1, for $T = 0$ (left pane) and $T = 0.01$ (right pane). These results are in accordance with Theorems 1-2. Figure 2 is obtained by zooming in on Figure 1 (right). Finally, Figure 3 shows the stability regions in the (T, τ) parameter space for $k = 12$ and $k = 25$, computed by the approach of Section III-C.

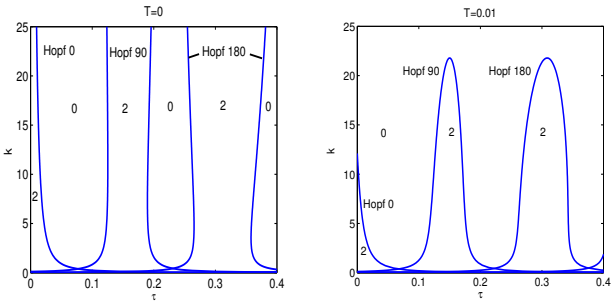


Fig. 1. Stability regions of synchronized equilibria of 4 coupled Lorenz systems in a ring configuration. The numbers refer to the number of characteristic roots in the closed right half plane. The Hopf bifurcation curves are classified based on type of emanating solution (32).

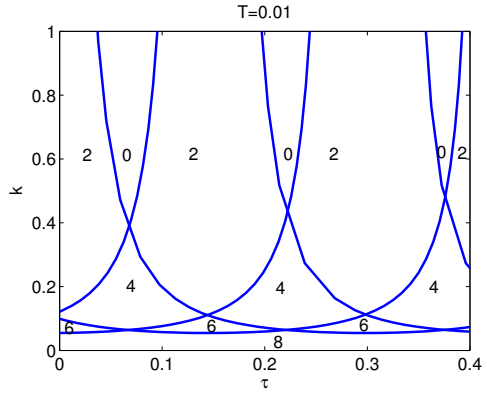


Fig. 2. Stability regions of synchronized equilibria of 4 coupled Lorenz systems in a ring configuration, for T=0.01.

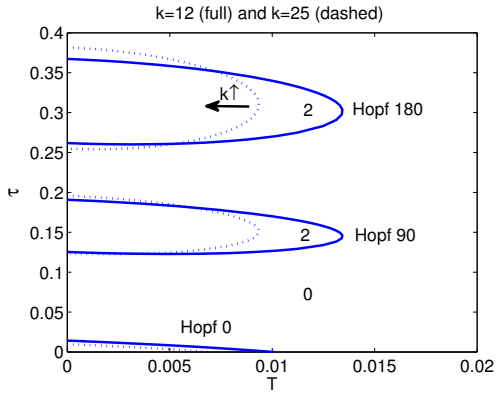


Fig. 3. Stability regions in the (T, τ) parameter space for $k = 12$ and $k = 25$.

V. Conclusion

We gained qualitative and quantitative insight in the synchronization of delay-coupled nonlinear oscillations, where the latency in the coupling is modeled by shifted gamma-distributed delays, by studying the stability regions of the synchronized equilibrium in the (coupling gain-delay) parameter space and by characterizing the structure of the emanating solutions in the bifurcations. Applying the results to the particular case of coupled Lorenz systems we have shown that, independently of the network topology, for sufficiently large coupling gains the distribution of the delay has a stabilizing effect on the stability of the synchronized equilibrium. The fact that the synchronization mechanism is a high-gain mechanism, based on dominating the destabilizing terms in the synchronization error dynamics, suggests that a similar conclusion can be drawn for other types of nonlinear oscillators.

References

[1] T. Insperger and G. Stépán. *Semi-discretization of time-dely systems*. Applied Mathematical Sciences. Springer, 2011.

[2] Y. Kuramoto. *Chemical Oscillations, Waves and Turbulence*. Springer, New York, 1984.

[3] N. MacDonald. *Biological delay systems: linear stability theory*. Cambridge University Press, Cambridge, 1989.

[4] W. Michiels, I.-C. Morărescu, and S.-I. Niculescu. Consensus problems with distributed delays, with application to traffic flow models. *SIAM Journal on Control and Optimization*, 48(1):77–101, 2009.

[5] W. Michiels and H. Nijmeijer. Synchronization of delay-coupled nonlinear oscillators: An approach based on the stability analysis of synchronized equilibria. *Chaos*, 19, 2009.

[6] I.-C. Morarescu, S.-I. Niculescu, and K. Gu. Stability crossing curves of shifted gamma-distributed delay systems. *SIAM Journal on Applied Dynamical Systems*, 6(2):475–493, 2007.

[7] I.-C. Morărescu, S.-I. Niculescu, and A. Girard. Consensus with constrained convergence rate and time-delays. In *IFAC Workshop on Time Delay Systems, TDS'10*, 2010.

[8] T. Oguchi, H. Nijmeijer, and T. Yamamoto. Synchronization in networks of chaotic systems with time-delay coupling. *Chaos*, 18, 2009.

[9] L. M. Pecora and T. L. Carroll. Master stability functions for synchronized coupled systems. *Phys. Rev. Lett.*, 80(10):2109–2112, 1998.

[10] S. H. Strogatz. *Nonlinear dynamics and chaos: with applications to physics, biology, chemistry and engineering*. Westview, Cambridge, 1994.

[11] S. H. Strogatz. *Sync: the emerging science of spontaneous order*. Hyperion Press, 2003.